

A Magnetic Bomb Scenario for Relativistic Jet Events in the Microquasar GRS 1915+105

Stephen S. Eikenberry¹ & Maurice H.H.M. van Putten²

ABSTRACT

We present a magnetic bomb scenario for the multiwavelength behavior during “Type B” relativistic jet events in the microquasar GRS 1915+105. These events are characterized by a hard X-ray dip which terminates in a soft X-ray spike. The scenario, based on the suspended accretion model for long gamma-ray bursts, posits a magnetic dynamo around an accreting Kerr black hole which reaches the Van Putten-Levinson critical value of poloidal magnetic field energy-to-kinetic energy ($\mathcal{E}_B/\mathcal{E}_k \simeq 1/15$) in the inner accretion disk. The toroidal inner accretion disk subsequently becomes unstable, and the poloidal magnetic field energy in the inner torus magnetosphere is promptly released as it disconnects from the black hole – the magnetic bomb (“B-bomb”) explosion. This scenario matches the long-duration time-scale and spectral evolution of the hard X-ray dip, and the short-duration time-scale and energetics of the soft X-ray spike of type B events, as well as correlated features in the infrared and radio wavebands. We discuss some implications of these results for understanding the formation of relativistic jets in black hole systems.

Subject headings: black hole physics – infrared: stars – stars: individual (GRS 1915+105) – X-rays: stars

1. Introduction

Since the initial discovery of their relativistic jets (Mirabel & Rodríguez (1994) ; Tingay, et al. (1995) ; Hjellming & Rupen (1995)), the Galactic microquasars have shown great potential as a laboratory for studying the formation of relativistic jets in black hole systems. These systems contain black holes of a few stellar masses, i.e.: $M_{BH} \simeq 7M_\odot$ for GRO 1655-40 (Orosz, et al. 1997) and $M_{BH} \simeq 14M_\odot$ for GRS 1915+105 (Greiner, et al. 2001), as opposed

¹Astronomy Department, University of Florida, Gainesville, FL 32611

²LIGO Project, NW17-161, 175 Albany Street, Cambridge, MA 02139-4307, USA

to the supermassive black holes of $\sim 10^8 - 10^9 M_\odot$ in quasars and active galactic nuclei. As a consequence, the timescales for variability are typically much shorter in microquasars, ranging from milliseconds to hours, as opposed to years to centuries in quasars and AGN. This allows studies of repeated patterns of jet-producing behaviors on timescales feasible for human investigation.

GRS 1915+105 is perhaps the most promising observational target for understanding the microquasar phenomenon, due to its continued violent activity in X-ray, infrared, and radio wavebands. Mirabel & Rodríguez (1994) first discovered relativistic jets in GRS 1915+105 through observations of oppositely-directed, collimated radio blobs moving with $v \simeq 0.92c$. Several years later, Fender et al., (1997) observed fast infrared (IR) flares and, later the same day, radio flares, hypothesized to be smaller-scale versions of the ejections seen by Mirabel & Rodríguez. Subsequent multiwavelength observations revealed a rich phenomenology of X-ray flares and dips, IR flares, and radio flares. This confirmed that GRS 1915+105 provided the first time-resolved observations of relativistic jet formation (Eikenberry, et al. (1998a); Eikenberry, et al. (1998b) ; Mirabel, et al. (1998) ; Fender & Pooley, (1999)).

GRS 1915+105 shows (at least) three types of jet-forming activities (Eikenberry, et al. 2001). The first of these, Type A, produces the major ejection events (Mirabel & Rodríguez 1994), and is associated with a reduction in hard X-ray flux on long timescales (Harmon, et al. 1997). The second of these types, Type B, shows smaller radio/infrared flares associated with X-ray dips/spikes (Eikenberry, et al. (1998a); Mirabel, et al. (1998)), and also exhibits apparent superluminal motions (Dhawan, et al. 2001). The third type, Type C, shows much fainter IR flares and associated radio flares with soft X-ray dips.

We present here a magnetic bomb scenario as a new mechanism for the multiwavelength behavior of Type B events. Our scenario is based on the suspended accretion model for long gamma-ray bursts (van Putten 2001) and the van Putten-Levinson stability criterion for magnetized disks (van Putten & Levinson 2003). This posits a rapidly spinning Kerr black hole (Kerr 1963) surrounded by a uniformly magnetized inner accretion disk, represented by *two counter-oriented current rings* which support a inner toroidal magnetosphere around the black hole, as well as an outer toroidal magnetosphere which extends to infinity. Prompt disconnection of the inner torus magnetosphere from the black hole releases magnetic energy in the form of radiation – a magnetic explosion (“B-bomb”). We shall quantify the energies and timescales of this mechanism, as well as the preceding evolution of build-up of the torus and its magnetosphere. This analysis describes a proposed two-state three-way “hole-torus-jet” connection in the low-hard dip state of Type B events. We note also that as we finished preparing this work for submission, Livio et al. (2003) have independently announced some very interesting, related work on a two-state “disk-jet” connection in GRS 1915+105.

The interaction of the black hole and the surrounding uniformly magnetized torus operates similarly to pulsar magnetospheres when viewed in poloidal topology. The inner face of the torus facing the black hole event horizon is equivalent to a pulsar, once we identify the event horizon of the black hole with a “compactified infinity” endowed with non-zero angular velocity (van Putten 1999). The geometry of this black hole and torus system viewed in poloidal cross-section shows a leading-order effect in the magnetic coupling (Figure 1), so that most of the black hole event horizon surface provides the asymptotic end point for the open magnetic field lines of the inner torus magnetosphere. A rapidly spinning black hole will rotate much faster than the inner accretion disk for nominal values of the disk radius. By the equivalence to pulsar magnetospheres described above, the torus and the black hole interact, whereby (a) most of the black hole spin energy is dissipated in the event horizon and (b) most of the black hole luminosity is incident onto the inner face of the torus (Figure 2).

In the weak magnetic field limit, extraction of energy from a Kerr black hole by a torque to surrounding matter in the accreting state is described by Ruffini & Wilson (1975). We appeal to the above equivalence to pulsars for the extension to the strong magnetic field-limit. This torque creates a “magnetic wall” around the black hole (van Putten & Levinson 2003) blocking passage of accreting material through the inner disk – a “suspended accretion” state (van Putten & Ostriker 2001) develops a torus as matter continues to build up by accretion in the extended disk. The black hole gradually spins down by conservation of energy and angular momentum.

Note that the equivalence to pulsar magnetospheres establishes causality in the extraction of black hole-spin energy by horizon Maxwell stresses, circumventing the criticism of Punsly & Coroniti (1990) to the force-free limit of Blandford and Znajek (1977) – see van Putten & Levinson (2003). Also, the field-lines connecting the black hole with the disk are equivalent to those on the outer face of the torus which extend to infinity and are open, not closed as claimed wrongly by (Li 2000). Closed field-lines in the inner and outer torus magnetosphere each form a toroidal ‘bag’ (van Putten 1999).

In §2 below, we describe the multiwavelength phenomenology of Type B events. In §3, we present the overall picture for the magnetic bomb scenario, based on the suspended accretion model for long gamma-ray bursts (van Putten 2001). In §4, we identify the time-scales, energetics and spectral evolution of the X-ray lightcurves in transition through a critical point of stability of the inner disk surrounding the black hole. In §5, we discuss the implications of this scenario for relativistic jet formation in GRS 1915+105 and future prospects for investigating its validity. Finally, in §6, we present our conclusions.

2. The Overall Multi-wavelength Pattern of Type B Events

Eikenberry, et al. (1998a) observed GRS 1915+105 on August 13-15, 1997 using the Proportional Counter Array (PCA) instrument of the Rossi X-ray Timing Explorer (RXTE), as well as an infrared camera mounted on the Palomar 200-inch telescope. As reported in Eikenberry, et al. (1998a) and Eikenberry, et al. (1998b), on August 14-15 GRS 1915+105 exhibited a complex, but repeating, pattern of X-ray activity associated with IR flares. The pattern begins with the onset of a spectrally-hard X-ray dip, shown in Figure 3, where the emission is dominated by a non-thermal power-law spectral component. This is the so-called “ β ” class of variability described by Belloni, et al. (2000). After a duration of $T_{dip} \sim 600$ s, the end of the dip is marked by a spectrally-soft X-ray spike, followed by a recovery to a higher count rate, which is dominated by thermal emission from the accretion disk (see e.g. Belloni, et al. (1997)). The X-ray lightcurve then transitions to an oscillating state characterized by rapid changes in the blackbody spectral component coupled with soft flares in the power-law component (Eikenberry, et al. 2000). Finally, a new hard dip begins.

Figures 4 and 5 show X-ray spectroscopic parameters for GRS 1915+105 during this time period. We extracted X-ray spectra in the $\sim 3-25$ keV range at a time resolution of 1 second. We applied standard procedures for response matrix generation for background estimation and subtraction, and corrected for PCA deadtime. We used the XSPEC v.11.2 software package to fit each spectrum with a standard model for black hole candidates consisting of a “soft” component modeled as a multi-temperature disk black body (e.g. Mitsuda, et al. (1984)) and a “hard” component modeled as a power-law, plus hydrogen absorption fixed to a column density of $6 \times 10^{22} \text{ cm}^{-2}$ (Muno, et al. 1999). We added a systematic error of 1% to each spectrum before the fit was performed. We obtained typical reduced chi-squared values $\chi^2_\nu \simeq 1.5$. (We present more detailed discussion of this behavior in Section 4.1.)

The lightcurve of the dip-terminating X-ray spike itself has several important features. The X-ray count rates rise to maximum on a timescale of $T_{spike} \sim 6 - 8$ seconds, and then fade rapidly away (Figure 6). During the spike, there are occasional episodes of rapid large-amplitude fading in the count rates, such as seen at the end of the spike shown in Figure 3 (Figure 7a). The timescales for such episodes are remarkably uniform. Whenever a drop of large enough amplitude ($> \frac{1}{e}$) is observed, it has an e-folding timescale of $\tau \sim 32$ ms (Figure 7b). After examining ~ 20 such fading episodes on 14 August 1997 and on 9 September 1997, we find a full range of $\sim 25 - 40$ ms for the e-folding timescales of these events. Based on the spectroscopic results above, the X-ray spikes are found to have typical X-ray fluences of $E_X \simeq 4 \times 10^{39}$ ergs.

The IR lightcurve (Figure 3b) shows large amplitude flares that begin near the end of the X-ray hard dip (Eikenberry, et al. 1998a). They are attributed to synchrotron emission

from a plasma blob ejected at relativistic speeds (Fender et al., (1997) ; Eikenberry, et al. (1998a); Mirabel, et al. (1998) ; Fender & Pooley, (1999) ; Dhawan, et al. (2001)), and similar to the larger ejections seen by Mirabel & Rodríguez (1994). The IR lightcurve also shows a much fainter excess associated with the oscillating portion of the X-ray lightcurve (Eikenberry, et al. 2000). The large IR flares reach their peak ~ 1200 seconds after the onset of the hard X-ray dip, or equivalently ~ 600 seconds after the X-ray spike. Mirabel, et al. (1998) and Fender & Pooley, (1999) also both observed associated radio flares delayed ~ 900 seconds from the IR flares. Invoking a simple model for synchrotron emission from an expanding plasma blob, Mirabel, et al. (1998) noted that the extrapolated time for the onset of the blob is near the time of the X-ray spike (see also Yadav (2001)).

3. The B-Bomb Scenario

We present here a magnetic bomb scenario associated with the formation and disruption of an accretion torus, and its similarly shaped magnetosphere, which accounts for the two time-scales of

$$T_{dip} \simeq 600\text{s}, \quad T_{spike} \simeq 6\text{s}, \quad (1)$$

the energetics, and the X-ray spectral evolution. This discussion is based on critical points of magnetic stability in the suspended accretion model for long gamma-ray bursts (van Putten (2001)). We first present a cartoon outline of this scenario, and then identify specific features in the observed lightcurves with physical events in the magnetic bomb scenario.

3.1. Cartoon Outline

We envision a rotating black hole and a thin accretion disk extending to somewhere near the last stable orbit (Figure 8a). As many have contemplated, a seed magnetic field in the accretion disk may develop a large-scale magnetic field by a dynamo process or, equivalently, winding of magnetic field-lines. For instance, in the magneto-rotational instability (MRI) of Balbus & Hawley, (1991), differential rotation in a Keplerian disk will shear magnetic loops, winding field lines and amplifying the magnetic field (Figure 8b).

We conjecture that this leads to the creation of a net poloidal magnetic flux, associated with an approximately uniform magnetization of matter in the inner accretion disk. This produces a toroidal magnetosphere around the black hole (Figure 8c). A torus magnetosphere around the black hole with net poloidal flux is represented by *two counter-oriented* current rings, concentric about the black hole (Figure 1). Through this current configuration, most

of the output of a rapidly rotating black hole in equilibrium with the surrounding torus magnetosphere satisfies (adapted from Thorne et al. (1986); van Putten (1999, 2001))

$$L_H \simeq 4 \times 10^{39} \left(\frac{\eta}{0.1} \right) \left(\frac{B}{3 \times 10^9 \text{G}} \right)^2 \left(\frac{M_{BH}}{14M_\odot} \right)^2 \text{ erg s}^{-1} \quad (2)$$

is incident on the inner face of the surrounding torus by the equivalence to pulsar magnetospheres viewed in poloidal topology (Goldreich and Julian 1969; van Putten 1999). Here, $\eta = \Omega_T/\Omega_H$ denotes the ratio of the angular velocity of the torus to that of the black hole, and B the strength of the poloidal component of the magnetic field. The MRI activity is initially driven by the power output of the black hole, L_H . The associated e-folding time for growth of the magnetic field energy is about 0.2 s (van Putten & Levinson 2003), whereby the magnetic field energy \mathcal{E}_B rapidly builds up to equilibrium values on the order of the kinetic energy \mathcal{E}_k of the torus on the time-scale of seconds. The magnetic field-energy ceases to grow in this equilibrium state (see (van Putten 2003) for a detailed calculation) – the dominant dissipation mechanism of the magnetic field is not well-known, but probably is associated with turbulent reconnection as considered in van Putten (2001).

In the weak magnetic field limit, a rotating black hole may provide a torque to surrounding matter in the accreting state (Ruffini & Wilson 1975). Recalling that most of the black hole power output is, in fact, incident on the inner face of a surrounding torus, we see that this creates a “magnetic wall” around the black hole (van Putten & Levinson 2003) blocking the passage of accreting material through the inner disk. This is the “suspended accretion” state (van Putten & Ostriker 2001). Matter then builds up in the torus at a rate determined by the rate of accretion in the extended disk (Figure 8d). As the mass in the torus increases, so does the associated equilibrium total magnetic field-energy \mathcal{E}_B . At the same time, the black hole gradually spins down by conservation of energy and angular momentum. This establishes causality in the extraction of black hole spin energy by horizon Maxwell stresses as proposed in (Ruffini & Wilson 1975; Blandford and Znajek 1977) – see also van Putten & Levinson (2003).

We here consider the possibility that this evolution reaches a critical point of instability, which triggers the prompt release of the stored magnetic energy \mathcal{E}_B – the “magnetic bomb” explosion (Figure 8e). We equate the total energy released with the energy \mathcal{E}_X in the observed X-ray spike. As individual field lines disconnect from their anchor point, poloidal magnetic field dissipates on a dynamical timescale. In this process, particles accelerate, producing X-ray emission from synchrotron, curvature, and inverse Compton processes. While individual field lines disappear quickly, the overall disconnection and release of energy over the entire region occurs in a sound crossing time. This is expected to be accompanied by outgoing shock fronts in the accretion disk. By continuing accretion from the outer disk, the system

gradually returns to our initial state (Figure 8f), and the cycle begins anew.

3.2. B-Bomb Features in the Lightcurves

Our cartoon highlights the following connections to the observations of Type B events.

The hard dips [$T_{dip} \simeq 600\text{s}$] represent the suspended accretion state – a uniformly magnetized torus pressing against a magnetic wall around the black hole (Figure 8d). Halting of accretion through the hot inner disk results in a dip in the X-ray lightcurve. The suspended accretion torus evolves on the long timescale of accretion towards increasing mass and associated magnetic field-strength. As shown in van Putten & Levinson (2003), this magnetic field reaches its equilibrium value on the time-scale of seconds when driven by input from the black hole. While the equilibrium magnetic field strength is not known ab initio, it is subject to a fundamental limit set by the condition of magnetic stability of the torus against buckling, given in terms of the Van Putten-Levinson criteria (van Putten & Levinson 2003)

$$\left. \frac{\mathcal{E}_B}{\mathcal{E}_k} \right|_c < 1/15 \quad (3)$$

of the poloidal magnetic field energy-to-kinetic energy. (Note that van Putten & Levinson (2003) also consider a tilt instability with a value of 1/12. Since these are similar values, we take the smaller limit here for simplicity.) In what follows, we express the critical magnetic field energy as

$$\mathcal{E}_B = \epsilon_B \mathcal{E}_k \quad (4)$$

where $\epsilon_B < 1/15$ corresponds to magnetic stability.

The X-ray spike [$T_{spike} \simeq 6\text{s}$] at the end of the dip corresponds to the disconnection event and the associated sudden release of the energy stored in the magnetic field (Figure 8e). This is triggered by instability of the inner torus magnetosphere, associated with violating the stability bound (3). The observed IR/radio synchrotron emission give considerable evidence for prompt jet ejecta from this disconnection event.

Recovery begins promptly following the spike, as the inner disk begins to refill the suspended accretion zone (Figure 8f). This accounts for the observed X-ray recovery phase.

4. Comparison with Observations

In the sections below, we discuss the detailed qualitative and quantitative features of the Type B events in the context of the magnetic bomb scenario, including spectral evolution,

timescales, and energetics.

4.1. X-ray Spectral Evolution

The X-ray spectral evolution observed from GRS 1915+105 during Type B events matches expectations for the magnetic bomb model. At the beginning of the hard dip, the blackbody temperature at the inner edge of the disk decreases as the disk inner radius itself expands (Figure 4). This behavior was first noted in GRS 1915+105 by Belloni, et al. (1997). The power-law emission component hardens at the same time. This is the initiation of the suspended accretion state, during which the torus mass and its associated kinetic energy and magnetic field-strength grow, increasing the energy stored in the “bomb”. As the inner edge of the optically-thick accretion flow moves to larger radii, the apparent inner radius of the disk is moved out with an accompanying temperature drop, in accordance with the observations.

The torus thus formed is connected to the extended accretion disk through a shock front. The formation of this shock in the accretion zone alters the non-thermal emission from the system, providing the observed hardening. The magnetic field in the inner region may also provide some additional non-thermal X-ray emission from synchrotron processes. The blackbody component quickly reaches an apparent equilibrium (although at the low temperatures of mid-dip, RXTE is not very sensitive to rather large changes in T_{disk} and R_{disk}), while the power-law index and normalization show some weak evolution. The inner radius of the disk (the boundary with the suspended accretion zone) is at $R \sim 150 - 200$ km. Note, however, that the radii inferred from the RXTE spectral fits should be viewed as approximations, with poorly known systematic correction factors.

As the inner torus magnetosphere becomes unstable, it disrupts and produces significant spectral evolution, notably the X-ray spike – representing the magnetic bomb explosion. At the onset of the spike, the inner disk radius begins to shrink and the blackbody temperature goes up (Figure 5). At the same time, the power-law normalization goes up, while the index remains constant at first. Once the spike reaches its peak and rapidly fades, the power-law index softens rapidly, and the normalization seems to stop its increasing trend momentarily, while the blackbody trends continue on. This behavior shows the infall of the suspended accretion zone boundary as the magnetic field strength decreases during the explosion. The power-law evolution during the spike is dominated by the explosion itself, and only after this fades away does the underlying “soft” component reveal itself. Note that after the spike has ended, the spectral evolution is essentially over – thus, the spike seems to reveal an actual state change in the X-ray emission of GRS 1915+105, rather than simply a momentary “blip”

in the lightcurve. This is confirmed explicitly by the analyses of similar events by Migliari & Belloni (2003).

Based on this correspondence, the magnetic bomb scenario seems compatible with the rather complicated X-ray spectral evolution of the Type B events.

4.2. B-Bomb Energetics and Timescales

The identification of certain observed features with counterparts in the magnetic bomb scenario also enables identification of timescales, particularly of the hard dip itself. We assume here that the observed energy release in the X-ray spike is equal to the magnetic energy stored in the bomb itself:

$$\mathcal{E}_B = \mathcal{E}_X, \quad (5)$$

where

$$\mathcal{E}_B = \frac{4}{3}\pi R^3 (B_{pol}^2/8\pi)f_B, \quad \mathcal{E}_X \simeq 4 \times 10^{39} \text{ ergs}. \quad (6)$$

Here, f_B is a filling factor of order unity which describes the volume of the inner torus magnetosphere as a fraction of $4\pi R^3/3$. In what follows, we shall take $f_B = 1$. The critical magnetic field-strength for stability of the torus satisfies (3), where $\mathcal{E}_k = M_{ID}M_{BH}/2R$. This gives

$$GM_{BH}M_{ID}/R = 2\epsilon_B^{-1}\mathcal{E}_X, \quad (7)$$

where $M_{BH} = 14M_\odot$ is the mass of the black hole and M_{ID} is the mass of the inner disk region in question. From the X-ray spectral fits, we see an apparent $R \sim 150 - 200$ km during long dips. Solving for M_{ID} , we derive an estimate of

$$M_{ID} \sim 8 \times 10^{20} \text{ g} (\epsilon_B/0.085)^{-1} \quad (8)$$

This is the amount of accreted matter needed to contain the magnetic bomb energy. We note that the mass (8) thus accumulated in a torus against the magnetic wall around the black hole satisfies

$$M_{ID} = \frac{4\pi}{3}\rho R^3 = 7.5 \times 10^{20} \text{ g} \left(\frac{\rho}{0.1 \text{ g/cm}^3} \right) \left(\frac{R}{6M} \right)^3 \left(\frac{M}{14M_\odot} \right)^3 \left(\frac{\epsilon_B}{0.0667} \right)^{-1}, \quad (9)$$

corresponds to an average density of about 0.1 g/cm^3 .

The torus builds up while matter accretes against the magnetic wall around the black hole. We can estimate the accretion rate \dot{M} from the X-ray luminosity during the accreting state, where $L_X \simeq 0.15\dot{M}c^2$ refers to a canonical value. Between the hard dips, GRS 1915+105 typically shows $L_X \simeq 1 \times 10^{39}$ ergs s⁻¹, giving $\dot{M} \sim 6 \times 10^{18}$ g s⁻¹. Set by the outer accretion disk, the accretion rate is continuous. Hence, $\tau_{acc} = M_{ID}/\dot{M}$ defines the time to build the torus in the suspended accretion state, i.e.:

$$\tau_{acc} \gtrsim 130 \text{ s} \left(\frac{\epsilon_B}{0.0667} \right)^{-1}. \quad (10)$$

This lower limit is in good agreement with the observed timescales $\sim 500 - 700$ s of hard dips.

As a cross-check on the energetics, we may rewrite (2) following the condition (5),

$$L_H \simeq 3 \times 10^{39} \left(\frac{\eta}{0.1} \right)^3 \left(\frac{\mathcal{E}_X}{4 \times 10^{39} \text{erg}} \right) \left(\frac{14M_\odot}{M} \right) \text{ erg s}^{-1} \quad (11)$$

as an upper bound in the limit of rapid rotation of the black hole. In the suspended accretion model, most of the black hole-luminosity L_H is incident onto the inner face of the torus, for reprocessing in magnetic winds and dissipation. Dissipation is due to turbulent magnetohydrodynamical flow, in response to competing torques on the inner and the outer face of the torus (van Putten 1999). These competing torques promote super-Keplerian and sub-Keplerian motions, and hence the torus assumes a geometrically thick shape. The modal power density spectrum of magnetohydrodynamical turbulence will be flat up to the first geometrical break in the azimuthal mode-number m , set by the ratio of the major-to-minor radius of the torus a/b (van Putten 2001, 2003). We may approximate the angular velocity distribution in the torus by $\Omega(r) = \Omega_T(R/r)^q$, where the rotation index $1.5 < q < 2$ is bounded between the Keplerian value and Rayleigh’s critical value for stability of the $m = 0$ mode. In this event, the balance equations describing the suspended accretion state give rise to a dissipation rate

$$P_d \simeq q \left(\frac{b}{R} \right) L_H < 0.27 \left(\frac{b}{M} \right) \left(\frac{\eta}{0.1} \right)^{3/2} \quad (12)$$

which is carried off in X-ray emissions, while the remainder of $L_{wind} = L_H - P_d$ is carried off in magnetic winds. (Here, b denotes the minor radius of the torus in the equatorial plane). These winds may in fact be the root source of the observed jets associated with the Type B events.

For GRS 1915+105 during the hard dips, we typically observe an X-ray luminosity $L_X \simeq 3 \times 10^{38}$ ergs s⁻¹. Our theoretical prediction of the upper bound $L_X \simeq 10^{39}$ erg s⁻¹

according to (12) and (11) is in good agreement with this observational constraint for rapidly rotating black holes, and nominal values $\eta \sim 0.1$ (corresponding to $R \simeq 7M_\odot$) and $b \simeq M$.

We also note that if the magnetic torus winds are baryon-rich (see Figure 2), they will decrease the effective \dot{M} during the suspended accretion state. According to (12), the observed X-ray luminosity during the hard dip $L_X[sas] \simeq 3 \times 10^{38} \text{erg s}^{-1}$ represents about 25% of the combined luminosity in X-rays and winds from the torus. Hence, we estimate $L_{wind} \simeq 1 \times 10^{39} \text{erg s}^{-1}$ for the torus wind. This may carry off matter at an approximate rate of $\dot{M}_{wind} = \frac{L_{wind}}{c^2}$, or $\dot{M}_{wind} = 3.3 \times 10^{18} \text{g s}^{-1}$. This would then revise our estimate of the time required to build the torus (10) to:

$$\tau_{acc} > 300 \text{ s} \left(\frac{\epsilon_B}{0.0667} \right)^{-1}. \quad (13)$$

This lower bound is again in agreement with the observed timescales $\sim 500 - 700 \text{s}$ of hard dips.

4.3. Timescales for the X-ray Spike

The spike itself shows two important timescales which can be explained under the magnetic bomb scenario. As noted above, the X-ray spike emission is identified with the disruption of the inner torus magnetosphere surrounding the black hole, releasing its magnetic energy on the dynamical timescale of the torus. The field lines should not all disconnect simultaneously, but rather over the sound speed crossing time of the inner disk region. That is, a single field line disconnects, creates a magnetosonic wave disturbance that propagates through the disk causing subsequent field lines to disconnect, and initiates a chain reaction propagating at the sound speed. For the limited ratio of magnetic-to-kinetic energy of the flows under consideration here, the magnetosonic speed is close to the sound speed. For a disk temperature of $\sim 0.5 \text{ keV}$, the corresponding sound speed is $c_s \sim 100 \text{ km/s}$. Thus, the sound crossing time over a diameter of $\sim 400 \text{ km}$ is $t_s \sim 4 \text{ seconds}$. Given the crude estimation we are making, this is a very close match to the $\sim 6 \text{s}$ duration of the X-ray spikes.

As the disconnection wave progresses, it encounters inhomogeneities in the B-field. Whenever there is an absence of field lines to detach and radiate, the observed X-ray flux should fade on the timescale of the radiative lifetime (approximately equal to the dynamical timescale) of the last detached field lines. For a radius of $\sim 200 \text{ km}$, the corresponding dynamical timescale for a black hole of $14M_\odot$ is $\sim 15 \text{ ms}$. The observed range in timescales for fading events during the spike is $\tau_s = 25 - 40 \text{ ms}$, corresponding to Keplerian radii of $R = 300 - 400 \text{ km}$. Again, for such crude estimation this is a very close match.

5. Discussion

This magnetic bomb scenario for GRS 1915+105, based on the more detailed suspended accretion model for gamma-ray bursts from rotating black holes (van Putten 2001), seems to provide a good match to many features in multiwavelength observations of Type B jet events. To our knowledge, it is the first such physical model to do so at the level of qualitative and quantitative lightcurve/timing features, spectral evolution, and the observed recurring timescales in the dips and spikes. Therefore, this physical framework seems to be a promising one within which to proceed in investigating the formation of relativistic jets in this system. However, there is still significant work to be done on this general scenario. Particular outstanding issues in the work mentioned above include the problem of creating net poloidal magnetic flux in forced shear flow and the radiative physics of prompt disconnection events of magnetospheres.

Furthermore, there are complex observational phenomena associated with the Type B events which we have not addressed here. For instance, Markwardt, et al. (1999) showed that 1-10 Hz quasi-periodic oscillations (QPO) are intimately linked to the system evolution during the hard dip (suspended accretion state in our model), and disappear outside the dip. This leads us to advance the notion that Type B events represent a magnetic flip-flop between a 'dirty' accreting state, corresponding to the observed oscillatory/fluctuating state, and a 'clean' suspended accretion state, corresponding to the observed long-duration and smooth hard-dip. We describe these states as follows:

(1) The dirty state is produced by an accreting inner disk of small radius with negligible or disordered poloidal magnetic field. The inner disk is turbulent and accretes on a viscous timescale. Only short-lived QPOs are allowed, by limited or short-range coherence in hydrodynamical wave-modes in the disk, whose convective motion spirals into the black hole.

(2) The clean state is produced by the suspended accretion state with a torus of extended radius and significant ordered poloidal magnetic field of about $10^9 G$. The torus develops on the viscous timescale of accretion, while it supports an inner torus magnetosphere of increasing magnetic energy. Long-lived QPOs are allowed (such as those of Markwardt, et al. (1999)), by large-scale coherence in wave-modes in the torus, whose convective motion forms closed circular orbits.

We attribute the transition from the accreting state to the suspended accretion state to a switch-on of poloidal magnetic flux. This transition is smooth and non-explosive. The timescale for pushing out the inner disk into the resulting torus is on the order of seconds, set by the black hole luminosity onto the inner disk. We have not determined the cause of the

appearance of such ordered magnetic field, or the trigger thereof. We attribute the transition from the suspended accretion state back to the “dirty” accreting state to a switch-off of the poloidal magnetic flux: our B-bomb scenario. The timescale for remnants of the torus to fall back and form an inner disk (of smaller radius) is a viscous timescale, possibly shortened by additional angular momentum loss in magnetic winds.

Other observational phenomena not treated here during these events include the fact that Type B infrared flares often show significant substructure (see e.g. Eikenberry, et al. (1998a)), spectral line evolution (Eikenberry, et al. 1998b), as well as extended low-level excesses (Eikenberry, et al. 2000). Given the link between the disconnection event (X-ray spike) and the launching of the long-wavelength flares under our scenario, we also expect that there may be some correlation between these IR flare properties and features in the X-ray spike.

We also mention here a conceivable link between the detailed observations and other models detailing various behaviors in GRS 1915+105 and microquasars in general. For instance, the Accretion Ejection Instability (AEI) model (Tagger & Pellat, 1999) shows some promise for explaining the 1-10 Hz QPO above in terms of a spiral shock wave in the disk (Rodriguez, et al. (2001) ; Varniere & Tagger, (2001)). Conceivably, our magnetic bomb scenario is compatible with a “magnetic flood” suggested in the context of AEI by Tagger, (2001). Furthermore, our scenario explains invokes a strong poloidal field component in the inner disk. Recent MHD models of relativistic jet formation in the innermost radii around a Kerr black hole consider a similar agent to produce powerful jets such as those observed in GRS 1915+105 (Koide, et al., 2002).

Finally, we point out that the timescale arguments above may be applicable to bomb models in general. Specifically, the X-ray spike duration (~ 6 s) corresponds to the sound crossing time for the inner disk region defined by the X-ray spectral fits ($R \sim 200$ km). In addition, the rapid fading timescale (~ 32 ms) observed during the spikes is similar to the dynamical timescale at this same radius. Finally, the energy released in the spike is equivalent to $\sim 10\%$ of the accretion energy accumulated during the duration of the hard X-ray dip immediately preceding it.

6. Conclusions

We have presented a magnetic bomb scenario for Type B relativistic jet events in GRS 1915+105, based on the more detailed suspended accretion state model of van Putten (2001) originally developed for gamma-ray bursts. This scenario posits episodic formation and

disruption of a torus and a similarly shaped magnetosphere in response to the interaction between a rotating black hole and the inner accretion disk.

The inner disk couples to the black hole, receiving energy and angular momentum from it. This results in a suspended accretion state, halting accretion through the (X-ray-emitting) innermost disk radii, and storing magnetic energy in the resulting torus. This is observed as the ~ 600 s hard X-ray dip. Once this energy level reaches a critical value, the inner disk and black hole disconnect through a magnetic buckling instability, and the stored magnetic energy is released – the “B-bomb” explodes. We identify the X-ray spike with the prompt disconnection of the inner torus magnetosphere. After the explosion, the inner disk refills and the cycle begins anew. This scenario provides general agreement with three observed timescales, energetics and spectral evolution in the X-ray waveband, as well as with key features in infrared and radio wavebands.

SSE is supported by an NSF CAREER grant (NSF-9983830), SSE thanks D. Rothstein for discussions and suggestions, and MVP thanks A. Levinson for discussions. The LIGO Observatories were constructed by Caltech and MIT with funding under cooperative agreement PHY 9210038. The LIGO Laboratory operates under cooperative agreement PHY-0107417. This paper has been assigned LIGO document number LIGO-P03xxxx-00-R.

REFERENCES

- Balbus,S.A. & Hawley,J.F. 1991, ApJ, 376, 214
- Blandford, R. D., and Znajek, R. L. 1977, MNRAS, 179, 433
- Belloni,T., Mendez,M., King,A.R., van der Klijs,M., van Paradijs,J. 1997, ApJ, 479, L145
- Belloni,T., Klein-Wolt,M., Mndez,M., van der Klis,M., van Paradijs,J. 2000, *å*, 355, 271
- Dhawan,V., Mirabel,I.F., Rodriguez,L.F. 2001, ApSSS, 276, 107
- Eikenberry,S.S., Bandyopadhyay,R.M. 2000, ApJ, 545, L131
- Eikenberry,S.S., Matthews,K., Morgan,E.H., Remillard,R.A., Nelson,R.W. 1998a, ApJ, 494, L61
- Eikenberry,S.S., Matthews,K., Muno,M., Blanco,P.R., Morgan,E.H., Remillard,R.A. 2000, ApJ, 532, L33
- Eikenberry,S.S 2001, ApSSS, 276, 101
- Eikenberry,S.S., Matthews,K., Murphy,T.W., Nelson,R.W., Morgan,E.H., Remillard,R.A., Muno, M. 1998b, ApJ, 506, L31
- Fender,R.P. & Pooley, G.G. 1998, MNRAS, 300, 573
- Fender,R.P., Pooley,G.G., Brocksopp,C., Newell,S.J. 1997, MNRAS, 290, L65
- Goldreich, P., and Julian, W.H. 1969, ApJ, 157, 869
- . Greiner,J., Cuby,J.G., McCaughrean,M.J. 2001, Nature, 414, 522
- Harmon,B.A, Deal,K.J., Paciesas,W.S., Zhang,S.N., Robinson,C.R., Gerard,E., Rodriguez,L.F., Mirabel,I.F. 1997, ApJ, 477, L85
- Hjellming,R.M. & Rupen,M.P. 1995, Nature, 375, 464
- Kerr, R.P., 1963, Phys. Rev. Lett.
- Koide,S., Shibata,K., Kudoh,T., Meier,D.L. 2002, Science, 295, 1688
- Li, L.-X., 2000, Phys. Rev. D., 61, 084016
- Livio, M., Pringle, J.E., & A.R.K. King, 2003, astro-ph/0304367

- Markwardt,C.B., Swank,J.H., Taam, R.E. 1999, ApJ, 513, L37
- Migliari,S. & Belloni,T. 2003, astro-ph 0303664
- Mirabel,I.F., Dhawan,V., Chaty,S., Rodriguez,L.F., Robinson,C., Swank,J., Geballe,T. 1998, A&A, 330, L9
- Mirabel,I.F. & Rodríguez,L.F. 1994, Nature, 371, 46
- Mitsuda, K., Inoue, H., Koyama, K., Makishima, K., Matsuoka, M., Ogawara, Y., Shibazaki, N., Suzuki, K., Tanaka, Y., & Hirano, T. 1984, PASJ, 36, 741
- Muno, M. P., Morgan, E. H. & Remillard, R. A. 1999, ApJ, 527, 321
- Orosz,J.A., et al. 1997, ApJ, 478, L83
- Punsly, B., & Coroniti, F.V., 1990, ApJ, 350, 518
- Reynolds, C.S., & Nowak, M.A., 2003, Phys. Rep., to appear
- Rodriguez,J., Varnire,P., Tagger,M., Durouchoux, Ph. 2001, ApSSS, 276, 235
- Ruffini, & Wilson, 1975, Phys. Rev. D
- Tagger,M.& Pellat,R. 1999, å, 349, 1003
- Tagger,M. 2001, ApSSS, 276, 113
- Thorne, K.S., Price, H.R., & McDonald D.A., 1986, The Membrane Paradigm (Yale University Press, New Haven)
- Tingay,S.J., et al. 1995, Nature, 374, 141
- van Putten, M.H.P.M., 1999, Science, 284, 115
- van Putten, M.H.P.M., & Ostriker, E.C., 2001, ApJ, 552, L31
- van Putten, M.H.P.M., 2001, Phys. Rep., 345, 1
- van Putten, M.H.P.M., 2003, ApJ, 583, 374
- van Putten, M.H.P.M., & Levinson, A., 2003, ApJ, 584, 937
- Varnire,P. & Tagger,M. 2001, ApSSS, 276, 233
- Yadav,J.S. 2001 ApJ, 548, 876

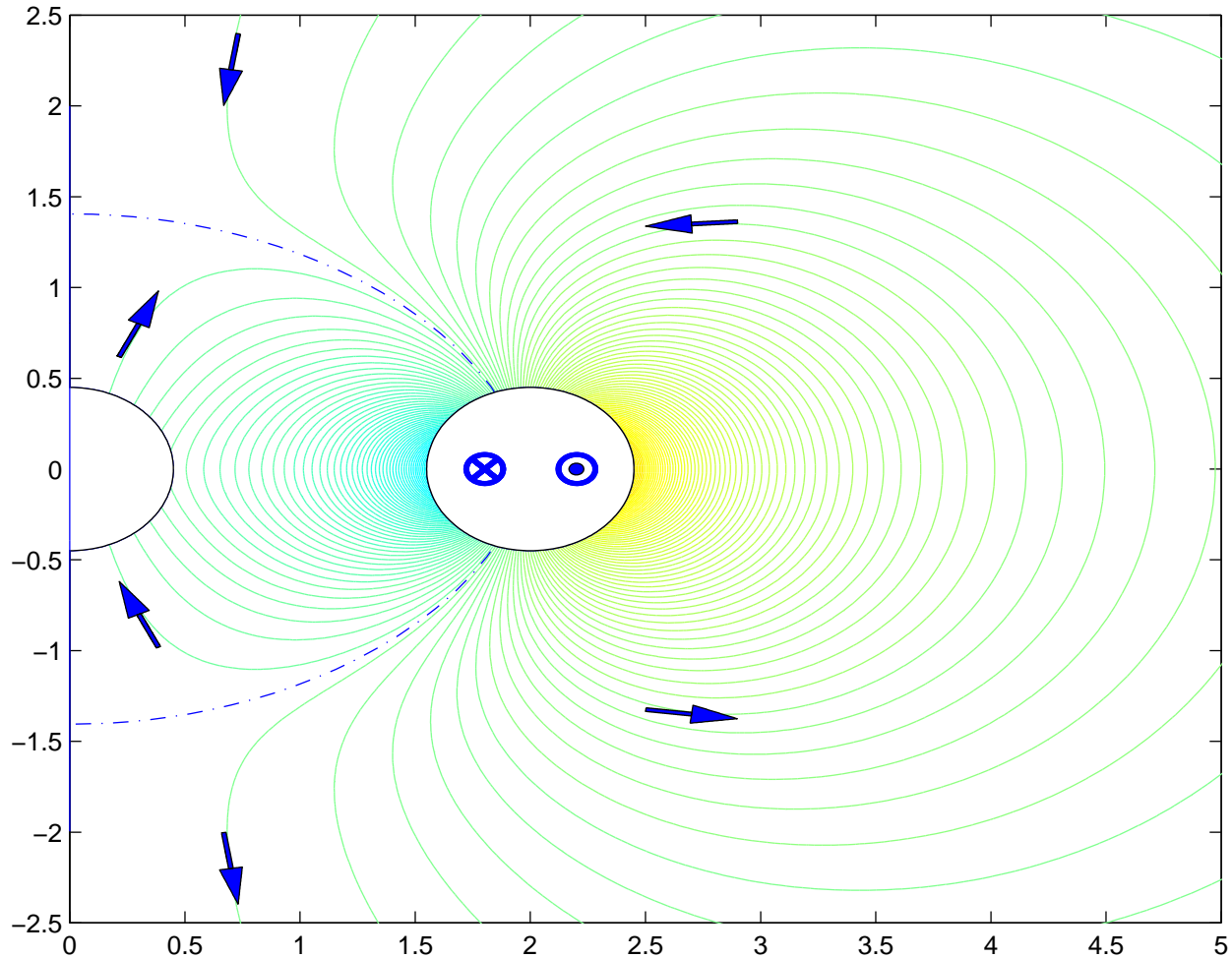


Fig. 1.— Numerical solution of the poloidal topology of magnetic flux-surfaces in vacuo and flat spacetime, produced by two concentric and oppositely oriented current rings in the torus (*center*) and a central current ring representing the equilibrium magnetic moment of the central object (*left*). The dashed line is the separatrix between the inner and the outer torus magnetosphere, associated with the inner and outer faces of the torus. A Kerr black hole develops a magnetic moment which preserves essentially uniform and maximal magnetic flux through its horizon in equilibrium with the surrounding torus magnetosphere. Torus winds, when sufficiently powerful, may alter the poloidal topology by creating a tube of open field-lines to infinity for baryon poor outflows from the black hole. (Reprinted from M.H.P.M. van Putten & A. Levinson, *The Astrophysical Journal*, 584, 937 (2003)).

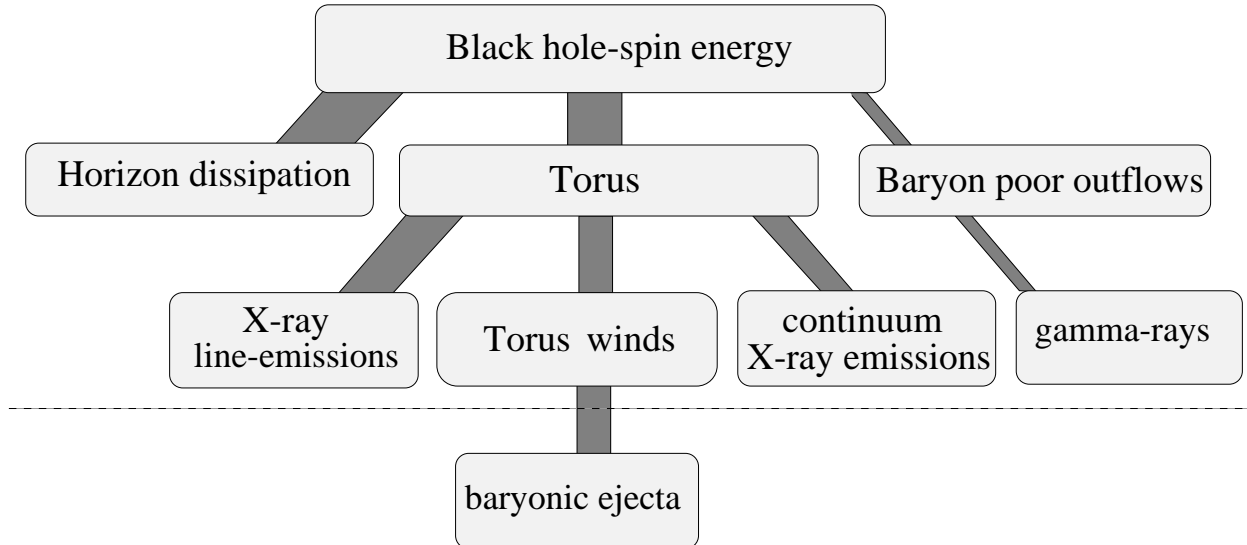


Fig. 2.— A radiation-energy diagram for the interaction of a Kerr black hole with a surrounding uniformly magnetized torus applied to GRS 1915+105, based on the suspended accretion model for GRBs from rotating black holes (van Putten 2001). The ratio of magnetic field energy-to-kinetic energy in the torus is subject to the van Putten-Levinson stability criterion $\mathcal{E}_B/\mathcal{E}_k < 1/15$ (van Putten & Levinson 2003). Most of the rotational energy is dissipated in the event horizon of the black hole, and this dissipation sets the lifetime of rapid spin of the black hole. Most of the black hole luminosity is incident onto the inner face of the torus for reprocessing into various channels, including thermal emissions, line-emissions (Reynolds & Nowak 2003), and build-up of poloidal magnetic field. The fate of torus winds is uncertain or unknown (below the dashed line), and may be related to baryonic ejecta and collimating winds. In the proposed B-bomb scenario, we identify observed energy release \mathcal{E}_X in soft X-rays in the short duration X-ray spike of Type B events with the dissipation of magnetic field-energy \mathcal{E}_B following prompt disconnection from the central black hole. The active lifetime of GRS 1915+105 for this behavior is actually set by the mass-donating star, since the magnetic field energy permits a lifetime of tens of Gyr for the rapid spin of the black hole.

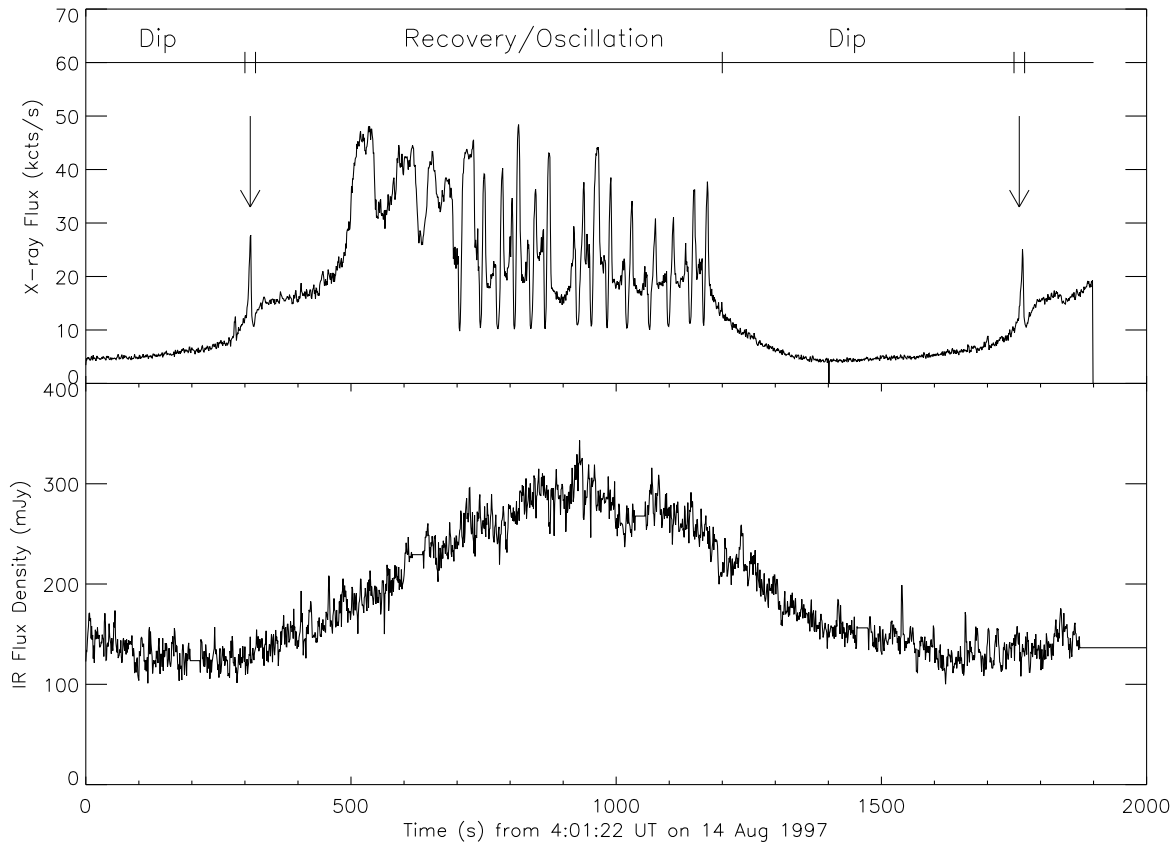


Fig. 3.— X-ray and IR observations of a Type B event based on the observations of Eikenberry, et al. (1998a). The timeline and labels at top show the various states described in the text, while arrows indicate the X-ray spikes. The typical Type B pattern begins with the onset of a spectrally-hard X-ray dip, where the emission is dominated by a non-thermal power-law spectral component. Near the end of the dip, there is a spectrally-soft X-ray spike, followed by a “recovery” ($t = 300 - 700$ s above) which is dominated by thermal emission from the accretion disk (see e.g. Belloni, et al. (1997)). The X-ray lightcurve then transitions into an oscillating state ($t = 700 - 1200$ s) characterized by rapid changes in the blackbody spectral component coupled with soft flares in the power-law component (Eikenberry, et al. 2000). Finally, a new hard dip begins ($t = 1200 - 1900$ s).

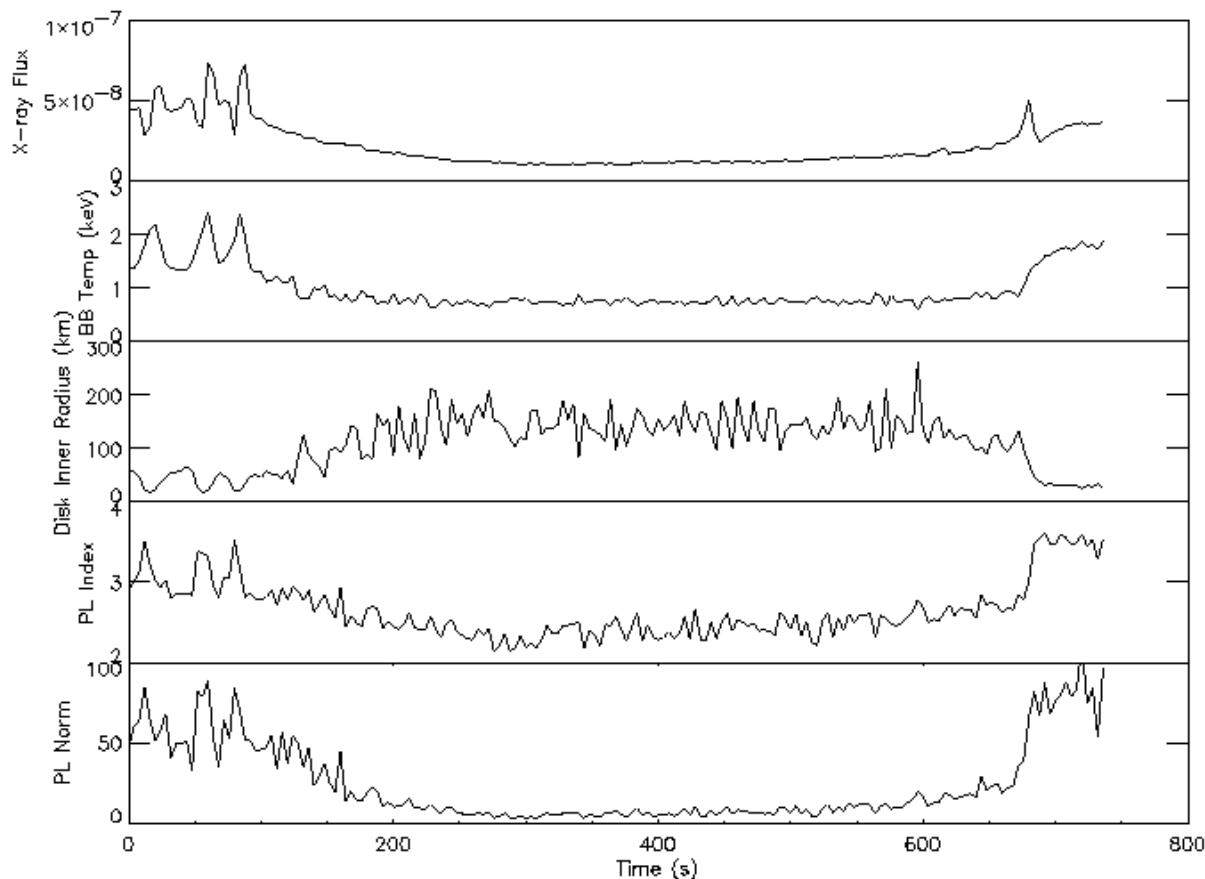


Fig. 4.— X-ray spectral evolution during a Type B event hard dip. Spectral fits are performed at 1-s time resolution to RXTE PCA data as described in Eikenberry, et al. (1998a). At the beginning of the dip, the inner accretion disk blackbody emission changes, with the temperature at the inner edge dropping while the radius of the inner edge increases dramatically. The power-law component hardens while its normalization drops. The dip terminates suddenly at the X-ray spike. Note that while the spike appears to have a short duration in the light curve, it actually reveals a dramatic “one-way” state change in the X-ray spectral properties.

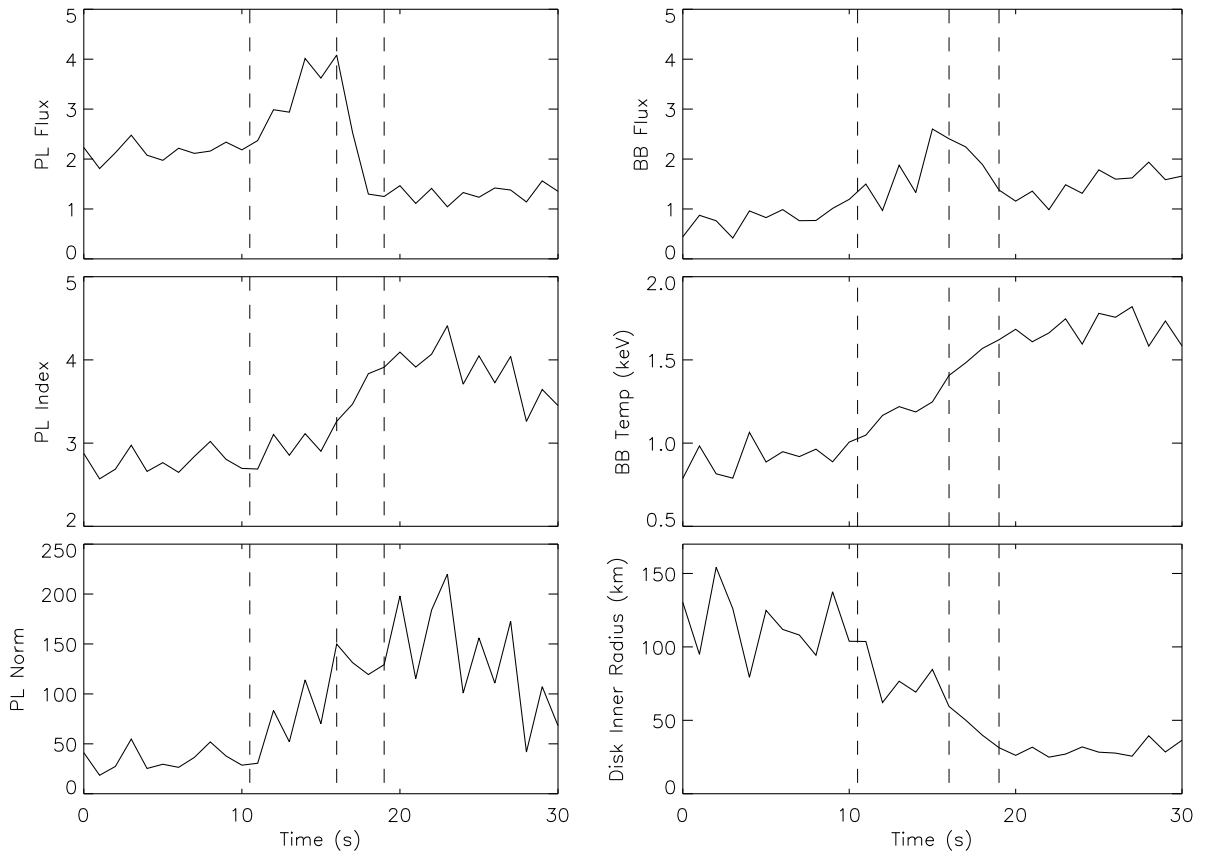


Fig. 5.— X-ray spectral evolution during an X-ray spike with 1-s time resolution. The first time tick indicates the beginning of the spike. The second the peak of the spike, and the third the end of the spike.

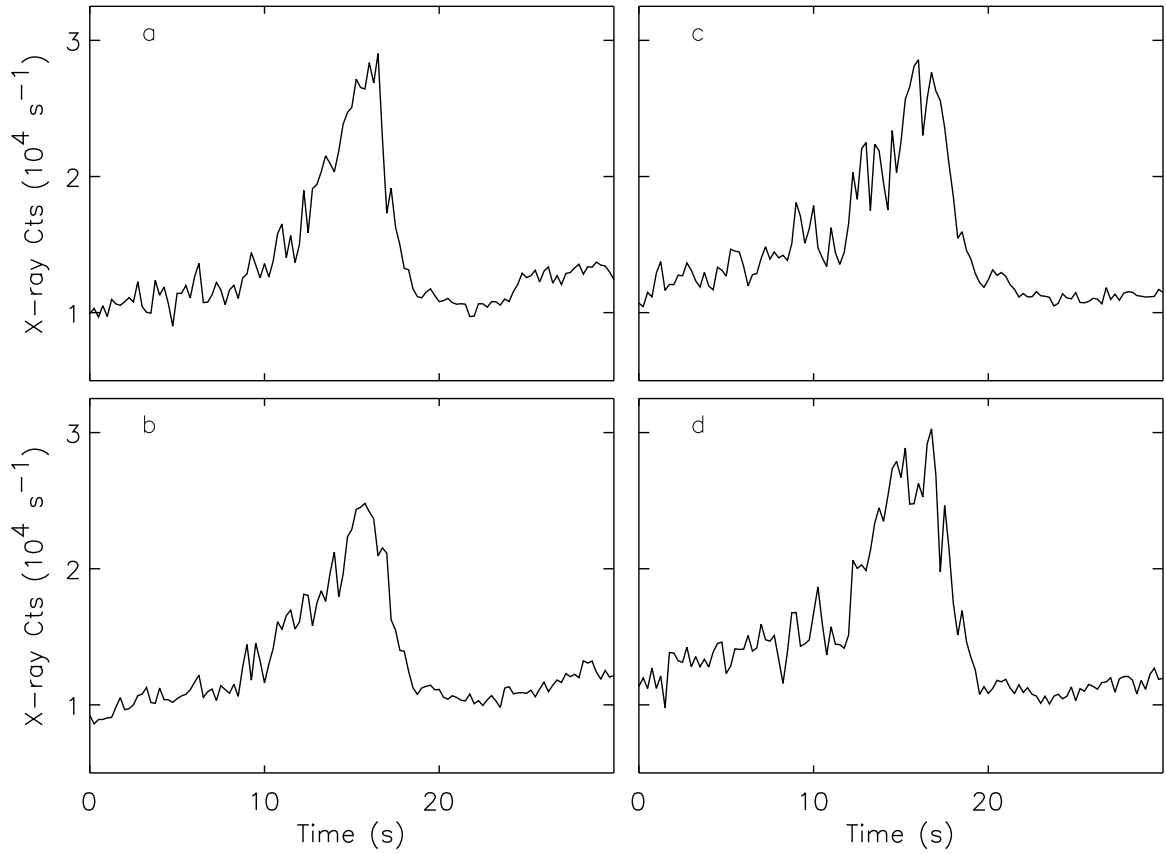


Fig. 6.— *Lightcurves of 4 X-ray spikes observed with the RXTE PCA on 14 August 1997. Note that the typical spike duration is $\sim 6-8$ s for essentially all of these spikes. In addition, there is statistically significant rapid (< 1 s) variability during the spikes themselves.*

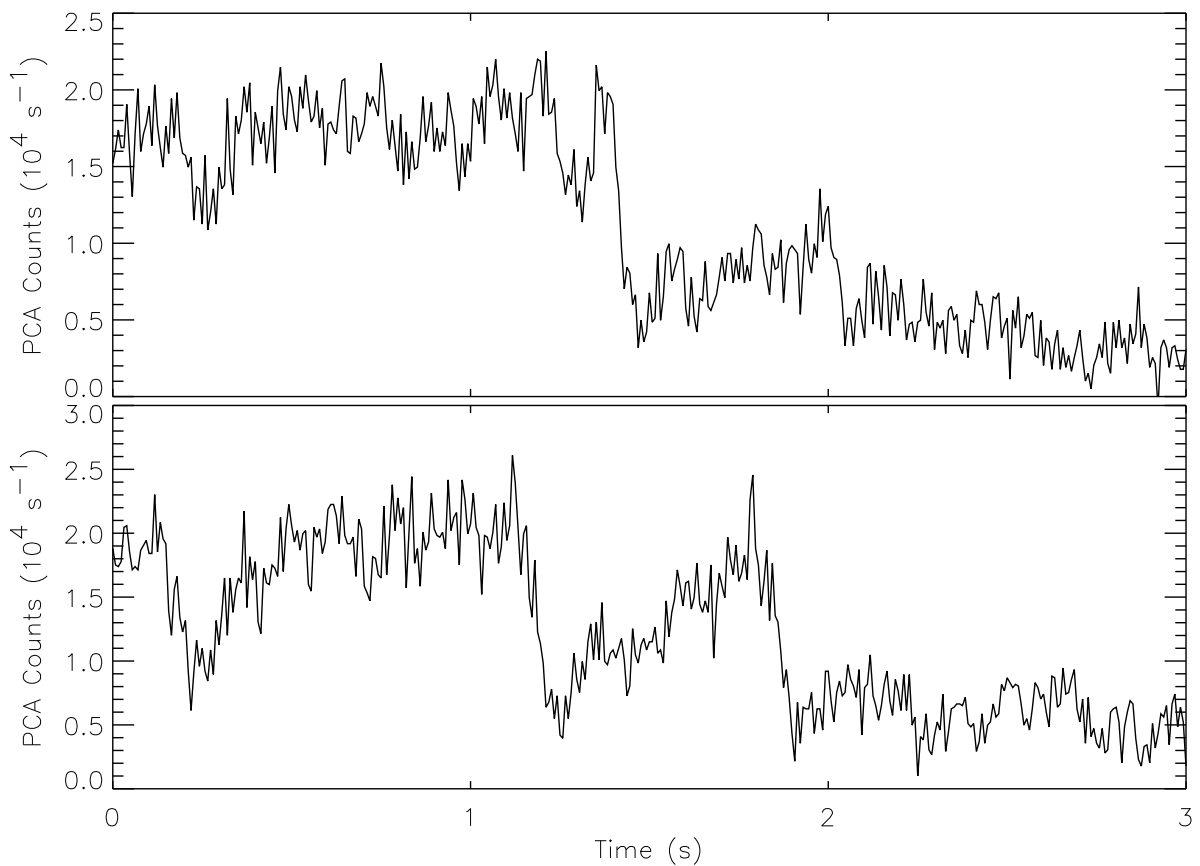


Fig. 7.— *High time-resolution (8-ms bins) PCA lightcurves of X-ray spikes from (a) Figure 4a (b) Figure 4d. Note the large-amplitude rapid fading events indicated by the arrows. All of the events with large fractional amplitudes ($\geq e$) and monotonic drops have e -folding timescales of $\tau \simeq 32$ ms.*

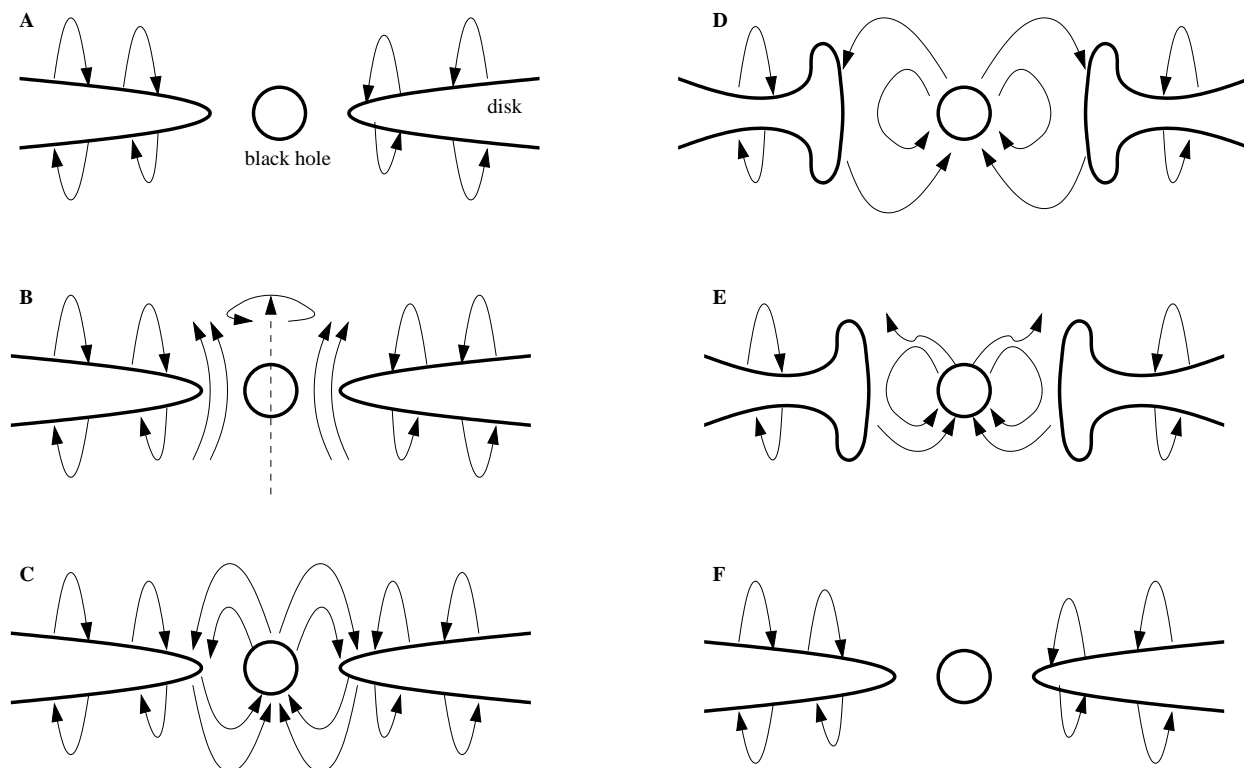


Fig. 8.— Cartoon of magnetic bomb evolution. The system begins with a thin accretion disk extending down to near the last stable orbit of a rotating black hole (A). Through a magneto-rotational instability, an ordered magnetic field develops and grows (B). Eventually, this field causes a connection between the inner accretion disk and the rotating black hole (C). This connection transfers energy and angular momentum from the black hole to the inner disk, suspending the accretion of material through the inner disk and producing a torus of material (D). When the ratio of magnetic energy to kinetic energy reaches the van Putten-Levinson instability criterion, the field disconnects and the stored magnetic energy is rapidly dissipated (the “B-Bom” – E). The inner disk then refills on a viscous timescale, and the system return to the initial state, allowing the cycle to begin anew (F).